

Tricritical behavior in a two-dimensional field theory

Herbert Hamber*

Department of Physics, University of California, Santa Barbara, California 93106

(Received 5 March 1979)

The critical behavior of a two-dimensional scalar Euclidean field theory with a potential term that allows for three minima is analyzed using an approximate position-space renormalization-group transformation on the equivalent quantum spin Hamiltonian. The global phase diagram shows a tricritical point separating a critical line from a line of first-order transitions. Other critical properties are examined, and good agreement is found with results on classical spin models belonging to the same universality class.

I. INTRODUCTION

Problems associated with phase transitions in two-dimensional field theories are currently being actively investigated. As one knows, these problems are directly linked by the transfer matrix¹ to corresponding field theories in one space and one time dimension. Thus insight gained from statistical mechanics regarding broken symmetries and correlations can provide a deeper understanding of the ground-state properties of the field theory. Alternatively, procedures for treating the quantum field theories give information on two-dimensional phase transitions.

In this paper we study a model whose degrees of freedom are described by a real scalar local field $\phi(x)$. The action of a given field configuration has the usual ϕ^4 form with a ϕ^6 term added to it. This allows for a situation in which the coefficient of the quartic term in the potential becomes zero or negative leading to three instead of two minimum energy configurations for the field. For such a ϕ^6 theory, mean-field theory predicts the existence of a tricritical point separating a critical line from a line of first-order transitions.² Here, we explore the properties of this ϕ^6 model using methods similar to those developed in treating the ϕ^4 problem.³

In Sec. II, the transfer Hamiltonian for the ϕ^6 problem is obtained. The theory is put on a one-dimensional lattice, keeping the Euclidean time direction continuous. While this clearly breaks the Euclidean covariance of the theory, one believes that it will be restored in the critical region, where the length scale is set by a diverging correlation length and the ultraviolet cutoff due to the finite lattice spacing is immaterial as far as the low-momentum properties of the system are concerned.⁴ The associated Hamiltonian defining the lattice theory splits into two parts, one describing the single-site problem and the other associated with the intersite coupling arising from the gradient term. Here we consider the situation in which the three localized states associated with the three minima of the potential will at a given

site provide a sufficient basis to describe the wave function at that site. Once the intersite coupling is also expressed in this truncated basis the Hamiltonian can be expressed as a one-dimensional spin-1 chain and the expectation values of monomials of the field are related to expectation values of powers of a spin matrix s_z .

In Sec. III, known results for various limiting cases of the spin-1 chain are discussed and a simple variational calculation for the ground state is carried out. This is equivalent to a mean-field treatment of the original statistical-mechanics problem. From the variational calculation a phase diagram is constructed. This phase diagram exhibits a tricritical point separating a critical line from a line of first-order transitions across which the expectation value of the order parameter changes discontinuously. By definition, at the tricritical point there is no effective four-point interaction and power counting shows that the most singular terms in a perturbation expansion around mean-field theory are generated by the ϕ^6 interaction, whose critical dimension is three. Therefore below three dimensions mean-field theory does not predict the right singular behavior as the critical points are approached.⁵

In order to study the modifications of the mean-field picture produced by the strong long-wavelength fluctuations an approximate renormalization-group analysis is carried out in Sec. IV. Here we study successive spin-1 chain Hamiltonians obtained by grouping two neighboring sites together, diagonalizing this two-site Hamiltonian and using its three lowest states to construct a new Hamiltonian describing a chain of coupled two-site blocks. This is similar to procedures previously developed for the spin- $\frac{1}{2}$ representation of a ϕ^4 theory.⁶ In Sec. VI this procedure is extended to blocks containing three sites. The results of the renormalization-group analysis are discussed in Sec. V.

We find a total of five fixed points leading to first- and second-order phase boundaries. The global phase diagram is determined by the topology of the

renormalization-group flows connecting the various fixed points. The critical exponents are obtained in the usual way by linearizing the renormalization-group equations in the neighborhood of the fixed points. These results are then compared with those derived in different classical spin models in two dimensions that belong to the same universality class and are believed to be represented by the same Euclidean action functional.

In Appendix A we show by using the transfer matrix technique how a class of classical spin models [the Blume-Emery-Griffiths (BEG) model⁷ for helium isotope mixtures in particular] is equivalent to our model which arose from the continuum-field theory. Appendix B contains the explicit derivation of the renormalization-group transformation.

II. THE MODEL

We consider an action functional for the real field $\phi(x_0, x_1)$ of the form

$$I[\phi] = \frac{1}{l} \int d^2x \left[\frac{1}{2} (\nabla \phi)^2 + \frac{1}{2} d_0 (\nabla \phi^2)^2 + U(\phi) \right], \quad (2.1)$$

with

$$U(\phi) = a_0 \phi^2 + b_0 \phi^4 + c_0 \phi^6. \quad (2.2)$$

In a field theory the real coefficients $a_0, b_0, c_0 > 0, d_0$ are the bare parameters and $l = \hbar$, while for a statistical-mechanical system the parameters will be functions of the temperature and l is kT . The generating or partition function is then given by the path integral

$$Z = \int \mathfrak{D}\phi e^{-I[\phi]}, \quad (2.3)$$

where $\mathfrak{D}\phi$ is a functional measure and the integration extends over all possible classical field configurations.

We now treat one direction as Euclidean time ($x_0 = \tau, x_1 = x$) and construct the equivalent Hamiltonian H . We introduce the momentum conjugate to the field ϕ

$$\pi(x) = i \frac{\partial \phi}{\partial \tau} \quad (2.4)$$

and get

$$H = \int dx \mathcal{H}(x), \quad (2.5)$$

$$\mathcal{H}(x) = \frac{1}{2} \pi^2(x) + \frac{1}{2} (\partial_x \phi)^2 + U(\phi). \quad (2.6)$$

The fields now obey equal time canonical commutation relations

$$[\phi(x, \tau), \pi(x', \tau)] = i \delta(x - x').$$

In going to the lattice we allow for the space variable x to become discrete and take the values $x_i = i/\Lambda$ where $1/\Lambda = a$ is the lattice spacing and i is an integer running from 1 to N . The length of the lattice is then $L = N/\Lambda$. To define the theory on the lattice we also make the replacements

$$\phi(x) \rightarrow \phi_i, \quad \pi(x) \rightarrow \Lambda p_i, \quad (2.7)$$

$$\partial_x \phi \rightarrow \Lambda (\phi_i - \phi_{i-1}), \quad (2.8)$$

$$\int dx \rightarrow \Lambda^{-1} \sum_i, \quad (2.9)$$

[where $\phi_i = \phi(x_i)$ etc.] and obtain the lattice Hamiltonian in terms of the canonical lattice variables

$$\frac{1}{\Lambda} H = \sum_{i=1}^N \left(\frac{1}{2} p_i^2 + a \phi_i^2 + b \phi_i^4 + c \phi_i^6 \right) - \sum_{i=1}^N \phi_i \phi_{i+1} - d \sum_{i=1}^N \phi_i^2 \phi_{i+1}^2. \quad (2.10)$$

Here $a = \Lambda^{-2} a_0 + 1, b = \Lambda^{-2} (b_0 + d_0), c = \Lambda^{-2} c_0$, and $d = d_0$ are dimensionless. We will mainly study the case $d = 0$.

As a next step we consider the single-site Schrödinger problem with the Hamiltonian

$$H_i = \frac{1}{2} p^2 + ax^2 + bx^4 + cx^6. \quad (2.11)$$

For $a, c > 0$ and $b \leq 0$ some of the possible potential configurations are shown in Fig. 1. When the potential barriers separating the three minima are large enough so that the tunneling matrix elements among the localized ground states of the separate wells are small, these localized states form a useful basis set for a description of the problem. Under the same conditions higher excitations at each lattice site can be neglected.⁸ In the Hilbert subspace spanned by these three states the Hamiltonian has the truncated matrix representation

$$H_i = \begin{pmatrix} \epsilon_0 & \omega & \omega \\ \omega & \epsilon_1 & \omega' \\ \omega & \omega' & \epsilon_1 \end{pmatrix}. \quad (2.12)$$

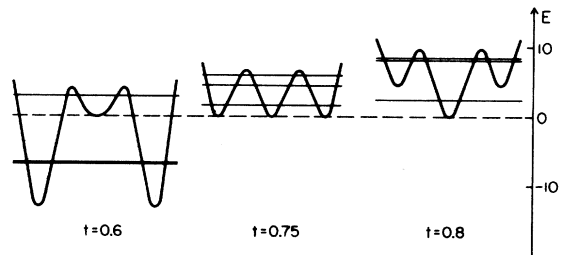


FIG. 1. Three possible configurations for the single-site potential, according to the value of $t = 3ac/b^2$ with $b = -4$ and $c = \frac{1}{4}$. The corresponding three lowest lying energy levels are shown in each case.

Here ϵ_0 and ϵ_1 are the ground-state energies of the separate inner and outer well, respectively. The tunneling matrix element between the two outer wells ω' is much smaller than the tunneling matrix element between adjacent wells: $\omega' \sim \omega^2 \ll 1$; ω depends exponentially on $ba^{1/2}/c$

$$|\omega| = \alpha \exp(-\text{const} \times ba^{1/2}/c) .$$

If we call the localized states $|+\rangle$, $|0\rangle$, and $|-\rangle$, the eigenvalues and eigenvectors of H_i have definite reflection symmetry, separating into two even-parity states

$$|\psi_{\pm}\rangle = \frac{1}{(1+b_{\pm}^2)^{1/2}} \left[\frac{1}{\sqrt{2}}(|+\rangle + |-\rangle) + b_{\pm}|c\rangle \right] , \quad (2.13)$$

$$b_{\pm} = -(2\sqrt{2}\omega)^{-1} \{ \epsilon_1 - \epsilon_0 + \omega' \mp [(\epsilon_1 - \epsilon_0 + \omega')^2 + 8\omega^2]^{1/2} \} , \quad (2.14)$$

with energy eigenvalues

$$\lambda_{\pm} = \frac{1}{2} \{ \epsilon_1 + \epsilon_0 + \omega' \pm [(\epsilon_1 + \omega' - \epsilon_0)^2 + 8\omega^2]^{1/2} \} \quad (2.15)$$

and an odd-parity state

$$|\psi_0\rangle = \frac{1}{\sqrt{2}}(|+\rangle - |-\rangle) , \quad (2.16)$$

with eigenvalue

$$\lambda_0 = \epsilon_1 - \omega' . \quad (2.17)$$

These eigenvalues are plotted in Fig. 2. As can be seen the odd-parity eigenvalue stays between the two even-parity ones ($\lambda_+ \geq \lambda_0 \geq \lambda_-$).

The single-site truncated Hamiltonian can now be rewritten in terms of spin-1 matrices with the up, down, and sideways states corresponding to the three retained states

$$H_i = \begin{pmatrix} \lambda_+ & 0 & 0 \\ 0 & \lambda_0 & 0 \\ 0 & 0 & \lambda_- \end{pmatrix}_i = \lambda_0 1 + \epsilon S_{z_i} + \epsilon' S_{z_i}^2 , \quad (2.18)$$

where

$$\epsilon = \frac{1}{2}(\lambda_+ - \lambda_-) , \quad (2.19)$$

$$\epsilon' = \frac{1}{2}(\lambda_+ + \lambda_-) - \lambda_0 . \quad (2.20)$$

The gradient term induces mixing between states of different parity, which is given in our approximation by the matrix elements

$$\begin{aligned} \langle \psi_+ | \phi_i | \psi_0 \rangle &= \langle \psi_0 | \phi_i | \psi_+ \rangle \\ &= \frac{\phi}{\sqrt{2}} \left[1 - \frac{\epsilon'}{\epsilon} \right]^{1/2} \equiv \delta_+ , \end{aligned} \quad (2.21)$$

$$\begin{aligned} \langle \psi_- | \phi_i | \psi_0 \rangle &= \langle \psi_0 | \phi_i | \psi_- \rangle \\ &= \frac{\phi}{\sqrt{2}} \left[1 + \frac{\epsilon'}{\epsilon} \right]^{1/2} \equiv \delta_- , \end{aligned} \quad (2.22)$$

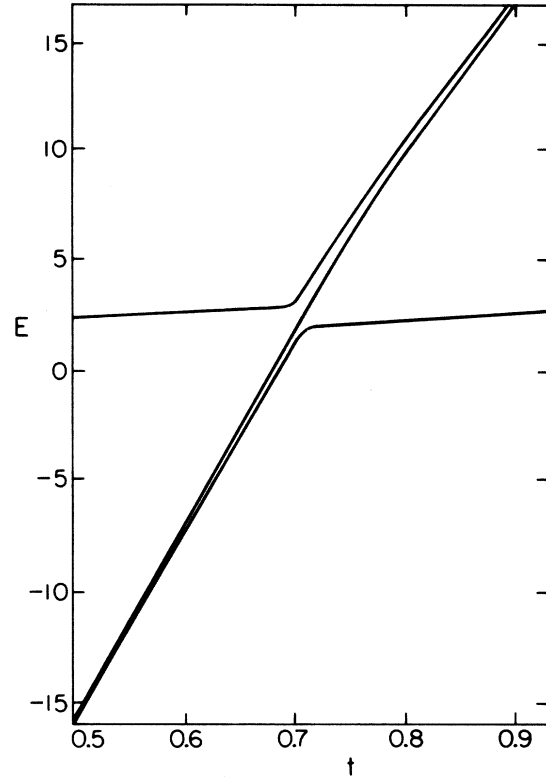


FIG. 2. Three lowest-energy levels λ_+ , λ_0 , and λ_- for the potential of Fig. 1 as a function of t .

where

$$\phi \equiv \langle + | \phi_i | + \rangle = -\langle - | \phi_i | - \rangle . \quad (2.23)$$

The Hamiltonian describing the bilinear interaction between lattice sites takes on the form

$$H_I = - \sum_i A_i A_{i+1} , \quad (2.24)$$

where

$$A_i = \begin{pmatrix} 0 & \delta_+ & 0 \\ \delta_+ & 0 & \delta_- \\ 0 & \delta_- & 0 \end{pmatrix}_i . \quad (2.25)$$

The interaction term biquadratic in the fields

$$-d \phi_i^2 \phi_{i+1}^2 \quad (2.26)$$

can also be easily written in matrix form in the truncated (definite parity) basis

$$-d \sum_i B_i B_{i+1} , \quad (2.27)$$

where

$$B_i = \begin{pmatrix} \eta_+ & 0 & J \\ 0 & \theta & 0 \\ J & 0 & \eta_- \end{pmatrix} \quad (2.28)$$

and

$$\eta_{\pm} = \frac{1}{2} \theta \left(1 \mp \frac{\epsilon'}{\epsilon} \right), \quad (2.29)$$

$$J = \frac{\theta}{2\epsilon} (\epsilon^2 - \epsilon'^2)^{1/2}, \quad (2.30)$$

$$\theta = \langle +|\phi_i^2|+ \rangle = \langle -|\phi_i^2|- \rangle. \quad (2.31)$$

In conclusion we have derived a matrix representation for the lattice Hamiltonian which is given by

$$\begin{aligned} \frac{1}{\Lambda} H = & \sum_i (\epsilon S_{z_i} + \epsilon' S_{z_i}^2) \\ & - \sum_i A_i A_{i+1} - d \sum_i B_i B_{i+1}. \end{aligned} \quad (2.32)$$

Here we have dropped the c -number term $\lambda_0 \sum_i 1_i$.

After reducing the interaction terms to diagonal form the Hamiltonian can also be written

$$\begin{aligned} \frac{1}{\Lambda} H = & \sum_i (\epsilon_1 S_{x_i} + \epsilon_2 S_{x_i}^2 + \epsilon_3 S_{z_i}^2) \\ & - \Delta \sum_i S_{z_i} S_{z_{i+1}} - k \sum_i S_{z_i}^2 S_{z_{i+1}}^2, \end{aligned} \quad (2.33)$$

with

$$\begin{aligned} \Delta = & \delta_+^2 + \delta_-^2 = \phi^2, \quad \epsilon_1 = \frac{2\epsilon}{\Delta} \delta_+ \delta_-, \\ k = & d\theta^2, \quad \epsilon_2 = \frac{\epsilon}{\Delta} (\delta_+^2 - \delta_-^2) + \epsilon', \\ \epsilon_3 = & \frac{2\epsilon}{\Delta} (\delta_+^2 - \delta_-^2), \end{aligned} \quad (2.34)$$

or equivalently

$$\epsilon_1 = \sqrt{2}\omega, \quad \epsilon_2 = 2\omega', \quad \epsilon_3 = \epsilon_1 - \epsilon_0 + \omega'. \quad (2.35)$$

Again a constant $-\epsilon_3 \sum_i 1_i$ was dropped. We define the two order parameters of the model to be

$$M = \langle S_z \rangle, \quad Q = \langle S_z^2 \rangle. \quad (2.36)$$

The spin Hamiltonian was derived for the case in which the tunneling matrix element ω is small. Thus $\omega' \sim \omega^2 \ll 1$. For consistency we will therefore be mainly interested in the case $\epsilon_2 \ll 1$. Furthermore the associated operator S_x^2 essentially duplicates the effect of the $\epsilon_1 S_x$ term.

H describes a one-dimensional array of quantum spin-1 objects coupled to each other by bilinear and biquadratic exchange terms and interacting with external transverse (ϵ_1) and crystal (ϵ_2, ϵ_3) fields. The Hamiltonian has the global symmetry with respect to $S_{z_i} \rightarrow -S_{z_i}$ at each site. The local symmetry of the single-site Hamiltonian is a consequence of the reflection symmetry of the potential $U(\phi)$. Both symmetries will be naturally preserved by the renormalization-group transformation described in Sec. IV.

III. CRITICAL BEHAVIOR IN MEAN-FIELD THEORY

From the considerations of Sec. II we are led to study the critical behavior of the truncated Hamiltonian

$$\begin{aligned} H = & \sum_i (x S_{x_i} + y S_{z_i}^2 + z S_{x_i}^2) \\ & - \sum_i S_{z_i} S_{z_{i+1}} - w \sum_i S_{z_i}^2 S_{z_{i+1}}^2, \end{aligned} \quad (3.1)$$

with

$$\begin{aligned} x = & \epsilon_1/\Delta, \quad z = \epsilon_2/\Delta, \\ y = & \epsilon_3/\Delta, \quad w = k/\Delta. \end{aligned} \quad (3.2)$$

Here we have rescaled the energy by Δ , since the critical properties depend only on the ratios of the original parameters. Then we have also absorbed the constant $(\Delta\Lambda)^{-1}$ into the definition of H . Unless otherwise stated we will be concerned here with the case $w=0$, corresponding to $d_0=0$ in the original partition function. Also, since we are mainly interested in $z \ll 1$, we will take z to be zero in the following. In this section we will first present some qualitative considerations regarding the possible phases of the Hamiltonian (3.1). We will then discuss some exact results concerning asymptotic forms of H and finally use a variational method to extract the mean-field critical properties.

We recall that the two order parameters are $M = \langle S_z \rangle$ and $Q = \langle S_z^2 \rangle$, where $\langle \hat{O} \rangle$ denotes the ground-state expectation value of the operator \hat{O} . Qualitatively we can discern three limiting cases and their associated phases: (i) $x, y \gg 1$: In this phase $M=0$, $Q \sim 0$, and the system is disordered. We will call this phase "para-0"; (ii) $x, |y| \gg 1$, $y < 0$: In this phase M is still zero but $Q \sim 1$. The system is partially ordered and we call the corresponding phase "para-1"; (iii) $x, |y| \ll 1$: This is the weak-coupling region corresponding to the ordered phase with $M \sim Q \sim 1$. This is the ferromagnetic ("ferro") phase in which the reflection symmetry $S_z \rightarrow -S_z$ is spontaneously broken. It will be shown in the following that (for small z and $w=0$) no phase boundary separates the para-1 and para-0 phase and that they are therefore part of a single paramagnetic phase. This is not expected to be the case in general. It should be pointed out that for $x=0$ (besides $z=w=0$) the model becomes classical since all dynamical variables then commute.

It is easy to derive some simple limiting forms of the spin model. In an asymptotic region to be specified below, the $w=0$ Hamiltonian reduces to a pure spin- $\frac{1}{2}$ Ising model in a transverse field.⁹ In order to see this we consider the first matrix form for H (2.32)

$$\frac{1}{\Lambda} H = \sum_i (\epsilon S_{z_i} + \epsilon' S_{z_i}^2) - \sum_i A_i A_{i+1}. \quad (3.3)$$

For $\epsilon - \epsilon' \ll 1$ we have $\delta_+ \sim 0$ and $\delta_- \sim \phi$ and A_i becomes

$$A_i = \phi \begin{pmatrix} 0 & 0 & 0 \\ 0 & 0 & 1 \\ 0 & 1 & 0 \end{pmatrix}_i . \quad (3.4)$$

The upper state $|\psi_+\rangle$ decouples and the Hamiltonian becomes (up to a constant)

$$\frac{1}{\Lambda} H = \sum_i \frac{1}{2} (\epsilon - \epsilon') \sigma_{zi} - \phi^2 \sum_i \sigma_{xi} \sigma_{xi+1} , \quad (3.5)$$

where σ_x and σ_z are the usual Pauli matrices. The spin- $\frac{1}{2}$ quantum Ising model is known to undergo a second-order phase transition at

$$\frac{1}{2} (\epsilon - \epsilon') = \phi^2 . \quad (3.6)$$

We therefore expect a second-order phase transition in the spin-1 model at

$$\frac{1}{2} x^2 \sim |y| , \quad y \ll 0 . \quad (3.7)$$

Furthermore it is possible to show that the model for $w \neq 0$, $z = \Delta = 0$, also reduces to a spin- $\frac{1}{2}$ quantum Ising model, but this time with an explicit symmetry breaking field. This circumstance is known in related spin models as Griffiths symmetry.¹⁰ To show this we consider again the first form for the spin Hamiltonian (2.32)

$$\frac{1}{\Lambda} H = \sum_i (\epsilon S_{zi} + \epsilon' S_{zi}^2) - d \sum_i B_i B_{i+1} . \quad (3.8)$$

We can write B_i

$$B_i = \theta 1_i + \begin{pmatrix} \eta_+ - \theta & 0 & J \\ 0 & 0 & 0 \\ J & 0 & \eta_- - \theta \end{pmatrix}_i . \quad (3.9)$$

Now we note that if we absorb the cross terms of $B_i B_{i+1}$ in the single-site Hamiltonian, we achieve a decoupling of the central ($|\psi_0\rangle$) state. Diagonalizing the interaction term and dropping constants yields

$$\begin{aligned} \frac{1}{\Lambda} H = \sum_i [(\epsilon^2 - \epsilon'^2)^{1/2} \sigma_x + (k/2 - \epsilon') \sigma_z] \\ - \frac{1}{4} k \sum_i \sigma_{zi} \sigma_{zi+1} . \end{aligned} \quad (3.10)$$

As anticipated, this is a spin- $\frac{1}{2}$ quantum Ising model in a transverse field $(\epsilon^2 - \epsilon'^2)^{1/2}$ and a longitudinal field $\frac{1}{2} k - \epsilon'$. The critical point corresponds to $\frac{1}{2} k - \epsilon' = 0$ and $(\epsilon^2 - \epsilon'^2)^{1/2} = \frac{1}{4} k$.

In order to get some more detailed quantitative information about the possible phases of the system we proceed to apply mean-field theory to the spin Hamiltonian, for the case $w = 0$. This information will later

be used for comparison with the phase diagram obtained from the renormalization-group analysis. In mean-field theory every spin feels only the average field due to neighboring fields and fluctuations are ignored. Within the Hamiltonian formulation of this problem, a mean-field-like solution is obtained by using a variationally determined wave function. For the normalized ground state that wave function is taken to be the product of N copies of the same single-site state

$$|\psi\rangle = \prod_i |\psi_i\rangle, \quad |\psi_i\rangle = \begin{pmatrix} \sin\phi \sin\theta \\ \cos\phi \\ \sin\phi \cos\theta \end{pmatrix}_i . \quad (3.11)$$

We proceed by minimizing the energy per site

$$\frac{1}{N} \langle \psi | H | \psi \rangle = E(\theta, \phi) , \quad (3.12)$$

where

$$\begin{aligned} E(\theta, \phi) = \sqrt{2} x \sin\phi \cos\phi (\sin\theta + \cos\theta) \\ + y \sin^2\phi - \sin^4\phi (1 - 2 \cos 2\theta)^2 . \end{aligned} \quad (3.13)$$

The variational equations that one needs to solve for all x and y are

$$\begin{aligned} 0 = \frac{\partial E}{\partial \theta} = \frac{x}{\sqrt{2}} \sin 2\phi (\cos\theta - \sin\theta) \\ + \frac{1}{2} (1 - \cos 2\phi)^2 \sin 4\theta , \end{aligned} \quad (3.14a)$$

$$\begin{aligned} 0 = \frac{\partial E}{\partial \phi} = \sqrt{2} x \cos 2\phi (\sin\theta + \cos\theta) + y \sin 2\phi \\ - \frac{1}{2} \sin 2\phi (1 - \cos 2\phi) (1 + \cos 4\theta) , \end{aligned} \quad (3.14b)$$

supplemented by the condition that the solutions of these coupled equations actually minimize $E(\theta, \phi)$. The two order parameters are then

$$M = \sin^2\phi (\sin^2\theta - \cos^2\theta) , \quad (3.15a)$$

$$Q = \sin^2\phi . \quad (3.15b)$$

It is possible to derive the equation for the second-order phase transition line analytically. The reason for this is that along the critical line M is vanishingly small. After some algebra one gets

$$x^2 = 2 - 2y - \frac{1}{8} y^2 \pm [(2 - 2y - \frac{1}{8} y^2)^2 - y^3]^{1/2} . \quad (3.16)$$

For $y \ll 0$ it assumes the limiting form

$$x^2 \xrightarrow{y \rightarrow -\infty} 4(-y + 4) + O(1/y) , \quad (3.17)$$

in agreement with the mean-field prediction for the Ising model critical point. It can be seen immediately that for $x = 0$ the system undergoes a first-order phase transition at $y = 1$ with a discontinuity of exactly 1 in both M and Q . Finally we observe that in the paramagnetic phase ($M = 0$) Q is continuous and has

the following functional dependence on x and y :

$$Q = \frac{1}{2} [1 - \text{sgn}(y) [1 + 2(x/y)^2]^{-1/2}] . \quad (3.18)$$

A numerical solution of the mean-field equations gives the phase diagrams shown in Figs. 4 and 5. As anticipated, there is only one paramagnetic phase, in agreement with results on related models.⁷ The system undergoes both first-order and second-order phase transitions. Because of the double valuedness of Q one gets two branches in the Q - x phase diagram (Fig. 5). The first-order line has become two phase-coexistence lines. The first-order line terminates at the tricritical point where it goes over into a critical line. M goes continuously to zero as the line is approached from the weak-coupling (or low-temperature) region. Q is continuous across this line and has the values given by the above analytical expression.

We have also studied the case $z \neq 0$. The overall features of the phase diagrams are unchanged. For small positive z the phase transition lines move slightly into the paramagnetic region. In Secs. IV–VI, we will analyze how these results change when the renormalization-group analysis is performed.

IV. RENORMALIZATION-GROUP TRANSFORMATION

In this section we analyze the low-momentum behavior of the system by means of a position-space renormalization-group transformation. The procedure, briefly outlined in the Introduction, is characterized by the following steps: (i) A few neighboring lattice sites are grouped into blocks. (ii) The Hamiltonian associated with this few-site problem is diagonalized, neglecting the interaction between sites belonging to different blocks. (iii) A subset of the lowest lying states of the block Hamiltonian are retained to be used as a new truncated basis set. The prescription for the choice of the lowest-lying states is dictated by the requirement that the block Hamiltonian assumes the same form as the site Hamiltonian. For example, if H is to be represented in terms of spin s matrices, a necessary but not sufficient condition for preserving the form of H is to keep the $2s + 1$ lowest states. By this procedure we eliminate higher-momentum states from the problem. (iv) The matrix elements of the interaction terms between blocks in the new truncated basis are evaluated. This will generate effective block-block interactions, which will still be nearest neighbor only. If the block Hamiltonian describes the same problem as the original Hamiltonian (i.e., same lattice type, spin kinematics, and functional form), then one has managed to change the length scale of the problem (by an amount that depends on the procedure one uses to

group sites into blocks) replacing at the same time the initial parameters in H by corresponding renormalized ones. In this way an approximate renormalization-group transformation is generated.¹¹ Once one has associated with every Hamiltonian the vector of its parameters, then each renormalization-group transformation can be thought of as a discrete jump of H in the parameter space. The succession of these jumps, obtained when the transformation is iterated, define the renormalization-group "trajectories" or "flows". From these the critical properties of the system can be read off.

Starting from general considerations it is possible to see under which conditions the spin Hamiltonian of Sec. III maintains its structure.

We first observe that the operator S_z is multiplicatively renormalizable. Since the matrices A_i (that appear when H is expressed in the definite parity basis) describing the intersite coupling mix even- and odd-parity states, they will have only nonzero matrix elements between states of different parity. This is because the block Hamiltonian is, as the site Hamiltonian, parity conserving. Therefore, if the ordering of the block energy levels starts with even-odd-even parity, then the symmetry of the truncated block states is the same as the symmetry of the single-site states, and A_i goes over into a matrix with the same structure. The change of basis that brought A_i into S_{z_i} will bring the new truncated matrix A_i into S_{z_i} up to a renormalization constant. We can therefore conclude that S_z is multiplicatively renormalizable.

On the contrary, S_z^2 is in general not expected to be multiplicatively renormalizable, and in fact it is not (see Sec. V). This implies that one should always add a term $z \sum_i S_{x_i}^2$ to the single-site part of the Hamiltonian in order to preserve its form under the renormalization group. Furthermore, the biquadratic exchange term $-w \sum_i S_{x_i}^2 S_{x_{i+1}}^2$ is also not expected to transform into itself (up to a multiplicative constant). Therefore the case $w \neq 0$ leads to a further enlargement of the parameter space. In the following we will study only the case $w = 0$.

We now construct a renormalization-group transformation. Following the above prescriptions we group two neighboring lattice points into a block. The Hamiltonian for the coupled two-site problem in the block b is

$$H_b = x(S_{x_1} + S_{x_2}) + z(S_{x_1}^2 + S_{x_2}^2) + y(S_{z_1}^2 + S_{z_2}^2) - S_{z_1} S_{z_2} . \quad (4.1)$$

The full lattice Hamiltonian (3.1) can now be written as made out of two parts, one describing the uncoupled blocks themselves (H_b) and the other their interactions (H_I)

$$H = \sum_b H_b + H_I . \quad (4.2)$$

Since we have grouped two lattice sites together in a block, we have $3^2=9$ states. We denote the states by $|\uparrow\uparrow\rangle \cdots |\downarrow\downarrow\rangle$.

H_b is reflection symmetric and symmetric under site interchange ($1 \rightleftharpoons 2$), and we therefore expect the eigenstates of H to share this symmetry. If we reexpress H in the basis of set of states that have definite transformation properties under these two symmetry operations, we see that H_b becomes block diagonal. The two invariant subspaces are the five-dimensional even-parity and the four-dimensional odd-parity subspace. The explicit form for the eigenvalues and eigenvectors is derived in Appendix B, together with the construction of the renormalization-group transformation.

When the three lower states alternate in parity (with an even state lying lowest), the functional form of the Hamiltonian is preserved when the blocks replace the sites. This condition is actually fulfilled in a reasonably large neighborhood of the tricritical region (see below). The recursion relation for the three parameters of H can be written, in general,

$$(x_{n+1}, y_{n+1}, z_{n+1}) = R(x_n, y_n, z_n) . \quad (4.3)$$

The change of scale at every step is here equal to 2, so that the n th iterate of H describes an effective Hamiltonian measured on a scale $a \times 2^n$, where a is the lattice spacing.

It is useful to look for the fixed points of R satisfying the property

$$R(x^*, y^*, z^*) = (x^*, y^*, z^*) . \quad (4.4)$$

At these points the Hamiltonian reproduces itself up to an additive constant. This signals the scale invariance of the theory: The correlation length is either infinite or zero. It is possible to find a subset of the fixed points of the recursion relations analytically. This is also shown in Appendix B. But in order to extract all the information available, the recursion relation must be studied numerically. Some of the renormalization-group flows obtained in this way are shown schematically in Fig. 3.

A detailed study of the recursion relations leads to a set of three fixed points which are inside the region of validity of our approximate truncation procedure (i.e., where the ordering of the three lowest energy states is of the form even-odd-even parity). The trivial fixed point Fe^* constitutes the sink for the ferromagnetic phase. It is a stable fixed point, and the correlation length there is zero. D^* is the discontinuity fixed point and satisfies the Nauenberg-Nienhuis criterion¹² for seeing a first-order phase transition in renormalization theory. T^* is the tricritical fixed point into which the tricritical point T of the $z=0$ theory is mapped, together with all the tricritical points for $z \neq 0$ lying on the line joining T and T^* . We are mainly interested, as stressed in Sec. III, in

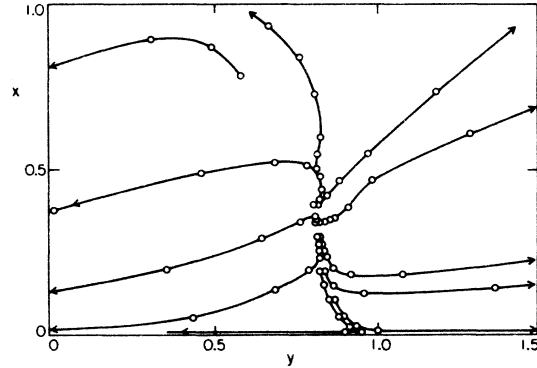


FIG. 3. Some renormalization-group flows are shown schematically in this figure. All the initial points are in the $z=0$ plane. The z direction is out of this plane.

the case $z \ll 1$. At the tricritical point the first-order phase transition line goes over into a continuous one. The first-order line constitutes the domain of attraction for the point D^* , whereas all points on the second-order line flow towards a critical fixed point.

Since our model reduces to the spin- $\frac{1}{2}$ Ising model for certain values of the parameters, (see Sec. III) we would expect to find a critical fixed point at a location corresponding to the critical point of the Ising model, if our renormalization-group transformation were exact. Because of the truncation procedure adopted, a crossing between the third and fourth level prevents us from solving the recursion relations in this asymptotic region. The same circumstance applies to the point in parameter space that acts as a sink for the paramagnetic phase.

The problems associated with the crossing of the energy levels could in principle be avoided in our framework by keeping more states at each site. This would destroy the simple form of the model and crossing between the fourth and fifth level is to be expected, but one might argue that by keeping more states one may progressively improve on the results. This has been shown for the spin- $\frac{1}{2}$ Ising model in a transverse field¹³ where it appears that the exact answer can be approached arbitrarily close if enough states are retained and blocks of more than two sites are used (see also Sec. V).

The critical exponents are obtained, as usual, by linearizing the recursion relation at the fixed point whose domain of attraction contains the transition point of interest. In our case the relation

$$\vec{k}' = R(\vec{k}), \quad \vec{k} = (x, y, z) \quad (4.5)$$

yields

$$k_\alpha - k_\alpha^* = T_{\alpha\beta}(k_\beta - k_\beta^*) , \quad (4.6)$$

with

$$T_{\alpha\beta} = \left(\frac{\partial k'_\alpha}{\partial k_\beta} \right)_{\vec{k}=\vec{k}^*} . \quad (4.7)$$

The eigenvalues λ_a of the matrix $T_{\alpha\beta}$ are related to the exponents y_a by

$$\lambda_a = b^{y_a}, \quad a = 1, 2, 3, \quad (4.8)$$

where $b=2$ is the length rescaling factor. The relevant eigenvalues $\lambda_a > 1$ give critical and tricritical exponents, and the results will be shown in Sec. V. Irrelevant eigenvalues give correction-to-scaling exponents.

V. RESULTS

The positions of the fixed points discussed in Sec. IV are listed in Table I, together with the coordinates of the tricritical point in the $z=0$ plane (T). The fixed points D^* and Fe^* are analytic results derived in Appendix B. The point C^* , and the fixed point that acts as a sink for the paramagnetic phase, lay outside the region of validity of our recursion relations because of crossing between the third and fourth energy level and its positions can be inferred from the renormalization-group flows in the region where our approximation is trustworthy. The phase diagram in the x - y plane (for $z=0$) that we obtain is shown in Fig. 4, together with the mean-field prediction. The slope of the critical line coincides with that of the first-order line at the tricritical point.

The order parameters M and Q are easily computed. M is evaluated by observing how the operator S_z gets renormalized after every iteration of the transformation. Since S_z is multiplicatively renormalizable, its renormalization constant is given at every step by $(\Delta_{n+1}/\Delta_n)^{1/2}$

$$(S_z)_R = \left(\frac{\Delta_{n+1}}{\Delta_n} \right)^{1/2} S_z . \quad (5.1)$$

TABLE I. Fixed points and the tricritical point in the $z=0$ plane, for $b=2$. Note that z^* differs from x^{*2} by less than 10% for T^* .

Fixed point	Type	RG location (x,y,z) , $b=2$
T^*	Tricritical	0.291 24, 0.894 46, 0.068 64
D^*	Discontinuity	0, 1, 0
Fe^*	Sink for ferro phase	0, -2, 0
T	Tricritical point for $z=0$	0.3234, 0.8338, 0

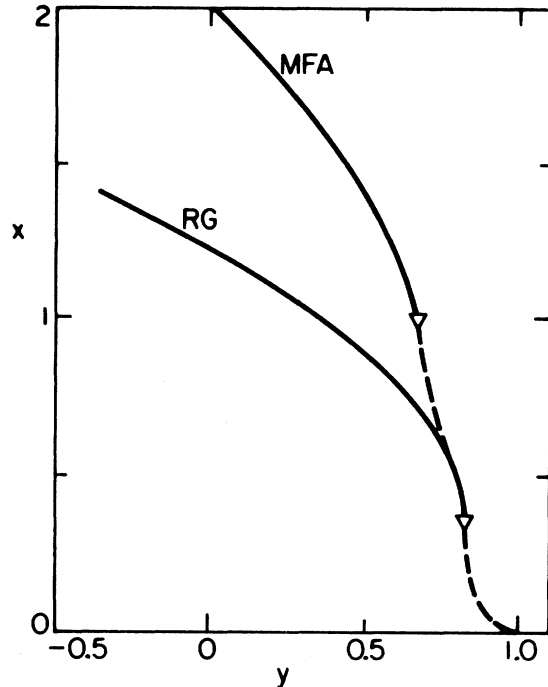


FIG. 4. Phase diagram in the x - y plane for $z=0$ as obtained from our renormalization-group analysis (RG). The result is compared with the mean-field (MFA) prediction. The tricritical point (∇) separates the first-order line (dashed) from the critical line (continuous).

Therefore M itself is given by

$$M = \lim_{n \rightarrow \infty} \prod_{i=0}^n \left(\frac{\Delta_{i+1}}{\Delta_i} \right)^{1/2} = \lim_{n \rightarrow \infty} \left(\frac{\Delta_n}{\Delta_0} \right)^{1/2} . \quad (5.2)$$

Knowledge of M around T^* can be used to determine the exponent β_T directly. Q can be evaluated by an analogous procedure. As stated before, S_z^2 is not multiplicatively renormalizable

$$(S_z^2)_R = Z_1^{(n)} S_z^2 + Z_2^{(n)} S_x + Z_3^{(n)} S_x^2 + Z_4^{(n)} 1 . \quad (5.3)$$

But we observe that after many (~ 20) iterations the operator S_z^2 is renormalized to a fixed matrix form, from which the value of Q can be read off. In our calculations the fixed form is always diagonal and either 1 or S_z^2 .

Therefore we have the two possibilities

$$Q = \lim_{n \rightarrow \infty} Z_1^{(n)} \quad (5.4)$$

or

$$Q = \lim_{n \rightarrow \infty} Z_4^{(n)} . \quad (5.5)$$

The first choice is pertinent to the ordered phase, where the effective spins are all aligned either up or down. The phase diagram in the Q - x phase, as obtained from our recursion relation, is shown in Fig. 5.

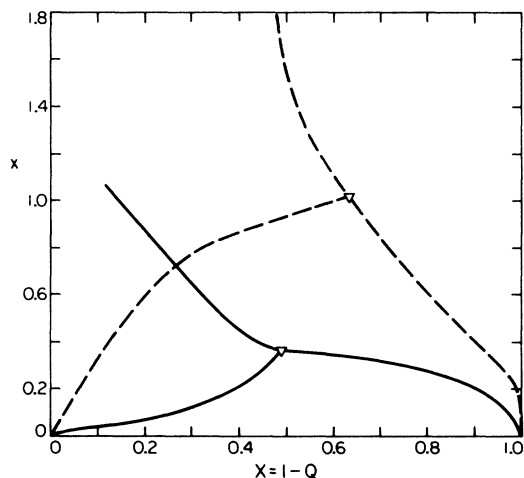


FIG. 5. Phase diagram for the theory in the Q - x plane in renormalization-group theory for $z=0$. The dashed line represents the mean-field result. The critical line terminates at the tricritical point (∇). The two lower lines going down to $x=0$ are coexistence curves bounding the two-phase region.

A direct quantitative comparison of our results with the results from the BEG model⁷ is not possible because of the ambiguity in identifying the temperature in the quantum spin model.

The results for the tricritical exponents are summarized in Table II, together with the exponents obtained from other models using different truncation procedures, which nevertheless should belong to the same universality class. We quote our results for the eigenvalues both for two-site ($b=2$) and three-site ($b=3$) blocks (see Sec. VI). The results for the latter case, which we expect to be more accurate, compare remarkably well with the results obtained from quite different models (although related by universality) to which an entirely different truncation procedure was applied (the agreement with the

results of Ref. 14 is better than 2%). We regard our results at roughly the same level of accuracy as the results for the ϕ^4 theory and the spin- $\frac{1}{2}$ Ising model in a transverse field.⁶ In the third column we list the results obtained from a renormalization-group analysis applied to the classical two-dimensional BEG model,¹⁴ whose relation to our model is shown in Appendix A. The fourth column contains the results for the classical spin- $\frac{1}{2}$ Ising antiferromagnet (with antiferromagnetic nearest-neighbor coupling and ferromagnetic next-to-nearest-neighbor coupling) also in two dimensions.¹⁵ We also compare with the predictions of the ϵ expansion¹⁶ (where $\epsilon=3-d$ and $n=1$ here) and with numerical (Monte Carlo) results.¹⁷

VI. IMPROVING THE ALGORITHM

In order to study the dependence of our results on the truncation procedure, we can resort to different methods. One possibility would be to retain more states in the truncation. This would of course lead to a block Hamiltonian which could not be written down in terms of spin-1 matrices. Nevertheless, one could study the problem in this larger basis in a similar manner. Clearly this would lead to an enlargement of the parameter space. Alternatively, one can group more lattice sites together in a block, keeping then only the three lowest lying states at every iteration. In this way the original form of H is preserved. If one uses both methods concurrently, one can achieve definite quantitative improvements in more simple models.

We now dissect the lattice into blocks of three sites and solve the uncoupled single-block Hamiltonian exactly, and construct then a renormalization-group transformation in a way that is completely analogous to what was done in Secs. I–V. In this case the length recalling factor is $b=3$. The jumps of the Hamiltonian in parameter space under the renormalization-group transformation are now com-

TABLE II. Tricritical eigenvalues and crossover exponent ϕ_T .

	$b=2$	$b=3$	BEG ^a	$s = \frac{1}{2}$ Ising ^b	$\epsilon = 3 - d$ expansion ^c	Monte Carlo ^d	MFA
y_{2T}	1.6613	1.8168	1.8373	1.825	1.968	1.36 ± 0.14	2
y_{4T}	0.6345	0.9321	0.9181	0.652	1.2	1.10 ± 0.22	1
y_{6T}	-0.8935	-0.6986	
ϕ_T	0.3819	0.5131	0.4997	0.357	0.6	0.81 ± 0.24	$\frac{1}{2}$

^aReference 14. RG on the classical 2-D BEG model.

^bReference 15. RG on the classical 2-D spin- $\frac{1}{2}$ Ising antiferromagnet, related by universality.

^cReference 16. ϵ expansion on the continuum-field theory, downwards from $d=3$.

^dReference 17. Monte Carlo study of the classical spin- $\frac{1}{2}$ Ising antiferromagnet in two dimensions.

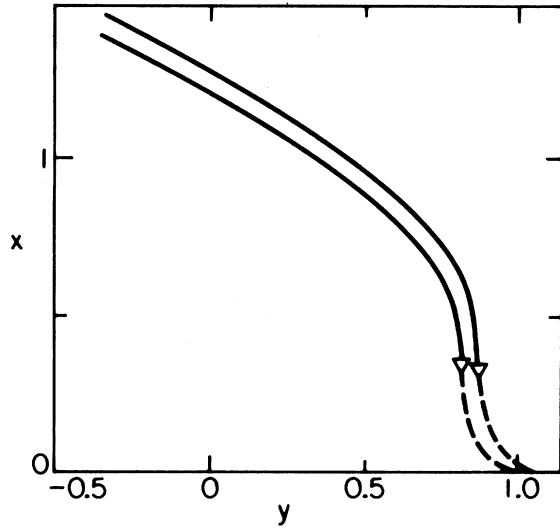


FIG. 6. x - y boundaries for initial values of $z=0$ (right curve) and $z=0.1$ (left curve) obtained from the three-site-block calculation. Around the tricritical point the agreement between the two-block (see Fig. 4) and the three-block prediction is equal to or less than 5%.

paratively bigger, for the same initial distance from the critical point.

The phase diagram that we compute in this case is shown in Fig. 6. When we compare the positions of the phase transition lines for $z=0$ in the $b=2$ and $b=3$ cases, we see that the agreement between the position of the two lines is better than 5% in the region shown. If the graph for $b=2$ and the one for $b=3$ were superimposed, the differences would hardly be notable on the scale chosen. In Table II we report the critical exponent as obtained in this case. The agreement with other calculations is, as mentioned before, quite encouraging.

ACKNOWLEDGMENTS

The author would like to thank Professor D. J. Scalapino and Professor J. Cardy for having suggested the problem and for many useful conversations, and R. Rendell for initial computer help. After this work was completed we learned that L. Masperi and D. Boyanovsky had performed similar calculations. This work was supported by the NSF under Contract No. DMR76-17373.

APPENDIX A: RELATION TO THE BEG MODEL

We consider the Blume-Emery-Griffiths (BEG) model on the square lattice ($d=2$). It is a spin-1

classical Ising model with the Hamiltonian

$$(J, K, \Delta) = \beta \left[-J \sum_{\langle ij \rangle} S_i S_j - K \sum_{\langle ij \rangle} S_i^2 S_j^2 + \sum_i (\epsilon S_i + q S_i^2) \right]. \quad (\text{A1})$$

Originally it was introduced to describe phase separation and superfluid ordering in ^3He - ^4He mixtures.

The partition function is given by

$$Z = \sum_{\text{configurations}} e^{-\mathcal{H}}. \quad (\text{A2})$$

Our aim is now to construct the associated quantum-mechanical Hamiltonian, by using the transfer matrix technique. For this purpose we identify one lattice direction as the (Euclidean) time axis. By an appropriate limiting procedure we will regard this direction as continuous and subsequently derive a class of models closely related to the one studied in Secs. I–VI of this paper.

We rewrite the above Hamiltonian in a form that will prove more convenient

$$\mathcal{H} = \beta \left[\frac{J}{2} \sum_{\langle ij \rangle} (S_i - S_j)^2 + \frac{K}{2} \sum_{\langle ij \rangle} (S_i^2 - S_j^2)^2 + \sum_i (h S_i + q' S_i^2) \right], \quad (\text{A3})$$

with

$$q' = q - J - K. \quad (\text{A4})$$

We now consider two neighboring rows of spins; the spins on the two rows will be denoted by S_n and σ_n . The transfer matrix will be defined as the quantum-mechanical imaginary-time evolution operator that carries information from one row to the next. The Hamiltonian for the two rows is

$$\mathcal{H}(s, \sigma) = \beta_z [\mathcal{H}(S) + \mathcal{H}(\sigma)] + \beta_t \left[\frac{J}{2} \sum_n (S_n - \sigma_n)^2 + \frac{K}{2} \sum_n (S_n^2 - \sigma_n^2)^2 \right] \quad (\text{A5})$$

and $\beta_z \mathcal{H}(S)$ is the Hamiltonian for a single chain

$$\beta_z \mathcal{H}(S) = \beta_z \left[\frac{J}{2} \sum_n (S_n - S_{n-1})^2 + \frac{K}{2} \sum_n (S_n^2 - S_{n-1}^2)^2 + \sum_n (h S_n + q' S_n^2) \right]. \quad (\text{A6})$$

We also have allowed for different couplings in the space (β_z) and time (β_t) directions.

It is easy to show that the partition function is the

trace of the N th power of a transfer matrix T , where the rows are labeled by the spin configuration of the first chain and the columns by those of the second neighboring chain. For N spins in a chain, there are 3^N possible spin configurations and therefore T has dimension 3^N .

The diagonal matrix elements of T are obtained by setting $S_n = \sigma_n$ for each n . Therefore

$$T_{\text{diagonal}} = e^{-2\beta_z \mathcal{K}(S)} . \quad (\text{A7})$$

The off-diagonal elements of T can be classified according to the amount of spins flipped. For n_1 spin flips with $\Delta S = 1$ and n_2 with $\Delta S = 2$ the matrix element of T is

$$T_{n_1 n_2} = e^{-\beta_z E(S, \sigma)} e^{-\beta_t [n_1(J+K) + 4n_2 J]/2} , \quad (\text{A8})$$

$$E(S, \sigma) = \mathcal{K}(S) + \mathcal{K}(\sigma) . \quad (\text{A9})$$

We now consider the limit of a highly anisotropic coupling

$$\beta_t \rightarrow \infty , \quad (\text{A10})$$

$$\frac{J}{2} \beta_z \rightarrow \lambda e^{-2\beta_t J} = \lambda \tau ,$$

with λ any real constant.

The limiting form for T becomes, when we neglect two spin flips with respect to one flip of either $\Delta S = 1$ or $\Delta S = 2$ ($n_1, n_2 = 0, 1$ but not $n_1 = n_2 = 1$)

$$T_{\text{diagonal}} = 1 + 2\beta_z \mathcal{K}(S) , \quad (\text{A11a})$$

$$T_{\text{off-diagonal}} = \begin{pmatrix} 0 & e^{-\beta_t(J+K)/2} & e^{-2\beta_t J} \\ e^{-\beta_t(J+K)/2} & 0 & e^{\beta_t(J+K)/2} \\ e^{-2\beta_t J} & e^{-\beta_t(J+K)/2} & 0 \end{pmatrix} , \quad (\text{A11b})$$

where we have neglected terms $O(\beta_z)$.

It is now possible to write T in terms of an infinitesimal generator H

$$T = 1 + \tau H + O(\tau^2) , \quad (\text{A12})$$

where we identify τ with $e^{-4J\beta_t}$, the infinitesimal lattice spacing along the Euclidean time direction. We get

$$H = \frac{4\lambda}{J} \mathcal{K}(S) + \sum_n (\sqrt{2} e^{-\beta_t(K-3J)/2} S_{x_n} + C_n) , \quad (\text{A13})$$

with

$$S_x = \frac{1}{\sqrt{2}} \begin{pmatrix} 0 & 1 & 0 \\ 1 & 0 & 1 \\ 0 & 1 & 0 \end{pmatrix} \quad (\text{A14a})$$

and

$$C = \begin{pmatrix} 0 & 0 & 1 \\ 0 & 0 & 0 \\ 1 & 0 & 0 \end{pmatrix} . \quad (\text{A14b})$$

The coefficient in front of S_x can be written

$$\sqrt{2}\tau^\alpha , \quad \text{with } \alpha = \frac{K-3J}{4J} . \quad (\text{A14c})$$

Therefore, for $\alpha > 0$ or $K > 3J$ we can drop the S_x term in H as $\tau \rightarrow 0$. For $K = 3J$ we keep it together with the other off-diagonal part given by C_n , and finally for $\alpha < 0$ or $K < 3J$ we redefine our limiting procedure as

$$\beta_t \rightarrow \infty , \quad (\text{A15})$$

$$\frac{J}{2} \beta_z \rightarrow \lambda e^{-\beta_t(J+K)/2} = \lambda \tau .$$

As a result we get that in this case we can neglect the C_n term in H as $\tau \rightarrow 0$.

We conclude therefore that we get three slightly different models, depending on whether $3J \leq K$.

When H is written entirely in terms of spin-1 matrices we have

$$H = \sum_i (\epsilon_1 S_{xi} + \epsilon_2 S_{xi}^2 + \epsilon_3 S_{xi}^2) - \Delta \sum_i S_{zi} S_{z(i+1)} - k \sum_i S_{zi}^2 S_{z(i+1)}^2 \quad (\text{A16})$$

and

$$\Delta = 2\lambda , \quad k = 2\lambda \frac{K}{J} ,$$

$$\epsilon_1 = 0, \quad \epsilon_2 = 2, \quad \epsilon_3 = \frac{4\lambda q}{J} \quad (K > 3J) , \quad (\text{A17})$$

$$\epsilon_1 = \sqrt{2}, \quad \epsilon_2 = 2, \quad \epsilon_3 = \frac{4\lambda q}{J} \quad (K = 3J) ,$$

$$\epsilon_1 = \sqrt{2}, \quad \epsilon_2 = 0, \quad \epsilon_3 = \frac{4\lambda q}{J} \quad (K < 3J) ,$$

This spin-1 quantum Ising model is expected to have the same critical behavior as the classical BEG model.

We therefore recover exactly the same model that was derived in Secs. I–VI from the continuum field theory. (The parameter k here has to be identified with the k of Sec. I–VI).

For $k = 0$ we obtain a relation between the parameters of the (anisotropic) BEG model and the parameters of the quantum Ising model

$$x = \frac{1}{\sqrt{2}\lambda}, \quad y = \frac{2q}{J}, \quad z \simeq 0 , \quad (\text{A18})$$

which can be used for comparing the phase diagrams in the two models (y is proportional to the chemical potential difference q for two-fluid systems).

APPENDIX B: DERIVATION OF THE RG TRANSFORMATION

As shown in Sec. IV, we first group two neighboring lattice points into a block and obtain the block Hamiltonian

$$H_{12} = \epsilon_1 (S_{x_1} + S_{x_2}) + \epsilon_2 (S_{x_1}^2 + S_{x_2}^2) + \epsilon_3 (S_{z_1}^2 + S_{z_2}^2) - \Delta S_{z_1} S_{z_2} . \quad (\text{B1})$$

The sites that have definite parity and have a definite symmetry under site interchange are

$$\psi_1^e = \frac{1}{\sqrt{2}}(|\uparrow\uparrow\rangle + |\downarrow\downarrow\rangle) , \quad (\text{B2a})$$

$$\psi_2^e = \frac{1}{\sqrt{2}}(|\uparrow\downarrow\rangle + |\downarrow\uparrow\rangle) , \quad (\text{B2b})$$

$$\psi_3^e = |\rightarrow\rightarrow\rangle , \quad (\text{B2c})$$

$$\psi_4^e = \frac{1}{2}(|\uparrow\rightarrow\rangle + |\downarrow\rightarrow\rangle + |\rightarrow\uparrow\rangle + |\rightarrow\downarrow\rangle) , \quad (\text{B2d})$$

$$\psi_5^e = \frac{1}{2}(|\uparrow\rightarrow\rangle + |\uparrow\rightarrow\rangle - |\rightarrow\uparrow\rangle - |\rightarrow\downarrow\rangle) , \quad (\text{B2e})$$

$$\psi_1^o = \frac{1}{\sqrt{2}}(|\uparrow\uparrow\rangle - |\downarrow\downarrow\rangle) , \quad (\text{B2f})$$

$$\psi_2^o = \frac{1}{\sqrt{2}}(|\uparrow\downarrow\rangle - |\downarrow\uparrow\rangle) , \quad (\text{B2g})$$

$$\psi_3^o = \frac{1}{2}(|\uparrow\rightarrow\rangle - |\downarrow\rightarrow\rangle + |\rightarrow\uparrow\rangle - |\rightarrow\downarrow\rangle) , \quad (\text{B2h})$$

$$\psi_4^o = \frac{1}{2}(|\uparrow\rightarrow\rangle - |\downarrow\rightarrow\rangle - |\rightarrow\uparrow\rangle + |\rightarrow\downarrow\rangle) . \quad (\text{B2i})$$

The superscript e indicates an even-parity state, and o indicates an odd-parity one. In this basis H_{12} becomes block diagonal. ψ_i^e is an eigenstate of H_{12} with eigenvalue $\lambda_i^e = 2\epsilon_2 + \epsilon_3$.

The odd-parity eigenvalues and eigenstates are easily written

$$\lambda_1^o = \frac{1}{2} [2\epsilon_2 + 3\epsilon_3 + \Delta + [(\epsilon_3 + \Delta)^2 + 4\epsilon_1^2]^{1/2}] ,$$

$$\phi_1^o = [1 + (a_1^o)^2]^{-1/2} (\psi_2^o + a_1^o \psi_4^o) , \quad (\text{B3a})$$

$$a_1^o = \frac{1}{\epsilon_1} (\lambda_1^o - \epsilon_2 - 2\epsilon_3 - \Delta) ,$$

$$\lambda_2^o = \frac{1}{2} [2\epsilon_2 + 3\epsilon_3 + \Delta + [(\epsilon_3 - \Delta)^2 + 4\epsilon_1^2]^{1/2}] ,$$

$$\phi_2^o = [1 + (a_2^o)^2]^{-1/2} (\psi_1^o + a_2^o \psi_3^o) , \quad (\text{B3b})$$

$$a_2^o = \frac{1}{\epsilon_1} (\lambda_2^o - \epsilon_2 - 2\epsilon_3 + \Delta) ,$$

$$\lambda_3^o = \frac{1}{2} [2\epsilon_2 + 3\epsilon_3 + \Delta - [(\epsilon_3 + \Delta)^2 + 4\epsilon_1^2]^{1/2}] ,$$

$$\phi_3^o = [1 + (a_3^o)^2]^{-1/2} (\psi_2^o + a_3^o \psi_4^o) , \quad (\text{B3c})$$

$$a_3^o = \frac{1}{\epsilon_1} (\lambda_3^o - \epsilon_2 - 2\epsilon_3 - \Delta) ,$$

$$\lambda_4^o = \frac{1}{2} [2\epsilon_2 + 3\epsilon_3 - \Delta - [(\epsilon_3 - \Delta)^2 + 4\epsilon_1^2]^{1/2}] ,$$

$$\phi_4^o = [1 + (a_4^o)^2]^{-1/2} (\psi_1^o + a_4^o \psi_3^o) ,$$

$$a_4^o = \frac{1}{\epsilon_1} (\lambda_4^o - \epsilon_2 - 2\epsilon_3 + \Delta) , \quad (\text{B3d})$$

$$\lambda_1^o \geq \lambda_2^o \geq \lambda_3^o \geq \lambda_4^o . \quad (\text{B4})$$

The even-parity eigenvalues are solutions of the quartic secular equation

$$(\epsilon_2 + 2\epsilon_3 - \Delta + \lambda) \{ (\epsilon_2 + 2\epsilon_3 + \Delta - \lambda) [(2\epsilon_2 - \lambda) (2\epsilon_2 + \epsilon_3 - \lambda) - 2\epsilon_1^2] - \epsilon_1^2 (2\epsilon_2 - \lambda) \} \\ - \epsilon_1^2 [(2\epsilon_2 - \lambda) (2\epsilon_2 + \epsilon_3 - \lambda) - 2\epsilon_1^2] - \epsilon_1^2 (\epsilon_2 + 2\epsilon_3 + \Delta - \lambda) (2\epsilon_2 - \lambda) = 0 . \quad (\text{B5a})$$

For $\epsilon_2 = 0$ the equation reduces to

$$[(2\epsilon_3 - \lambda)^2 - \Delta^2] [\lambda(\lambda - \epsilon_3) - 2\epsilon_1^2] \\ + 2\epsilon_1^2 \lambda (2\epsilon_3 - \lambda) = 0 . \quad (\text{B5b})$$

The solutions of the above quartics can be found analytically. We call the eigenvalues $\lambda_1^e, \lambda_2^e, \lambda_4^e, \lambda_5^e$; $\lambda_1^e \geq \lambda_2^e \geq \lambda_4^e \geq \lambda_5^e$.

The even-parity eigenstates are easily obtained once the eigenvalues are known. Their general form is

$$\phi_i^e = \frac{1}{N_i} (\psi_1^e + a_i^e \psi_2^e + b_i^e \psi_3^e + c_i^e \psi_4^e) , \quad (\text{B6a})$$

with

$$N_i = (1 + a_i^{e2} + b_i^{e2} + c_i^{e2})^{1/2} \quad (\text{B6b})$$

and a_i^e, b_i^e, c_i^e functions of the associated eigenvalues λ_i^e ; $i = 1, 2, 4, 5$.

In the tricritical region, where the three lowest eigenstates are two even-parity with one odd-parity

state in between, we can use as a truncated basis

$$|+\rangle = (1 + a_+^2 + b_+^2 + c_+^2)^{-1/2} \\ \times (\psi_1^e + a_+ \psi_2^e + b_+ \psi_3^e + c_+ \psi_4^e) , \quad (\text{B7a})$$

$$|0\rangle = [1 + (a_0^o)^2]^{-1/2} (\psi_1^o + a_0^o \psi_3^o) , \quad (\text{B7b})$$

$$|-\rangle = (1 + a_-^2 + b_-^2 + c_-^2)^{-1/2} \\ \times (\psi_1^e + a_- \psi_2^e + b_- \psi_3^e + c_- \psi_4^e) , \quad (\text{B7c})$$

$$(a^+ = a_4^o, a^- = a_5^o, \text{ etc.}) .$$

From these eigenvalues and eigenvectors the new Hamiltonian generated by our iteration procedure can be constructed. The new parameters can be obtained from the formulas (2.18) to (2.34) of Sec. II. Some fixed points of the recursion relations can be found analytically. Consider the point $x=0, y=1, z=0$. Measured on the scale of Δ the eigenvalues are $\lambda_+ = 1, \lambda_o = 1, \lambda_- = 0$. Therefore $a_{04} = -1$ and

$$b_- \sim \infty, a_+ = b_+ = c_+, b_-/c_- = b_-/a_- \sim \infty .$$

From this one has $\epsilon_1' = \epsilon_2' = 0$ and $\epsilon_3' = \Delta' = 1$. This

shows that the point

$$D^* = (0, 1, 0) ,$$

is a fixed point. (The renormalization-group analysis performed in Sec. IV shows that D^* is the discontinuity fixed point).

Also the point $x=0, y=-2, z=0$ can be shown analytically to be a fixed point. In this case

$$\lambda_+ = -3, \lambda_0 = -5, \lambda_- = -5 ,$$

and

$$a_{04} = 0, \quad a_+/c_+ \sim \infty ,$$

$$a_+/b_+ \sim \infty, \quad a_- = b_- = c_- = 0 .$$

This gives $\epsilon'_1 = \epsilon'_2 = 0$ and $\Delta' = 1, \epsilon'_3 = -2$. Thus the vector

$$Fe^* = (0, -2, 0)$$

is also a fixed point (in fact, the weak-coupling or low-temperature fixed point).

*This work forms part of a thesis fulfilling part of the requirements for the Ph.D. degree of the author.

¹T. Schultz, D. Mattis, and E. Lieb, *Rev. Mod. Phys.* **36**, 856 (1964); D. J. Scalapino, M. Sears, and R. A. Ferrell, *Phys. Rev. B* **6**, 3409 (1972); E. Fradkin and L. Susskind, *Phys. Rev. D* **17**, 2637 (1978).

²L. Landau (1937). Reprinted in *Collected Papers by L. Landau*, edited by D. ter Haar (Pergamon, New York, 1965).

³S. Drell, M. Weinstein, and S. Yankielowicz, *Phys. Rev. D* **16**, 1769 (1977). Related unpublished work was independently carried out by R. Pearson, S. Jafarey, D. J. Scalapino, and B. Stoockly. See also J. L. Cardy, *Nucl. Phys. B* **115**, 141 (1976).

⁴K. G. Wilson and J. Kogut, *Phys. Rep. C* **12**, 75 (1974).

⁵E. Reidel and F. Wegner, *Phys. Rev. Lett.* **29**, 349 (1972).

⁶See Ref. 3 and A. Fernandez-Pacheco, SLAC-Pub-2099 (unpublished).

⁷M. Blume, V. J. Emery, and R. B. Griffiths, *Phys. Rev. A* **4**, 1071 (1971), and references cited therein. For a vectorialized version, see J. L. Cardy and D. J. Scalapino,

Phys. Rev. B **19**, 1 (1979); A. N. Berker and D. Nelson, *Phys. Rev. B* (to be published).

⁸Y. Imry and D. J. Scalapino, *Phys. Rev. A* **9**, 1672 (1974).

⁹P. Pfeuty, *Ann. Phys. (N.Y.)* **57**, 79 (1970).

¹⁰R. B. Griffiths, *Physica (Utrecht)* **33**, 689 (1967).

¹¹L. P. Kadanoff and A. Houghton, *Phys. Rev. B* **11**, 377 (1975); K. G. Wilson and J. Kogut, *Phys. Rep. C* **12**, 75 (1974).

¹²M. Nauenberg and B. Nienhuis, *Phys. Rev. Lett.* **35**, 477 (1975).

¹³M. Weinstein (private communication).

¹⁴A. N. Berker and M. Wortis, *Phys. Rev. B* **14**, 4946 (1976); see also T. W. Burkhardt, *Phys. Rev. B* **14**, 1196 (1976).

¹⁵M. Nauenberg and B. Nienhuis, *Phys. Rev. B* **13**, 2021 (1976).

¹⁶T. S. Chang, G. F. Tuthill, and H. E. Stanley, *Phys. Rev. B* **9**, 4882 (1974).

¹⁷D. P. Landau, *Phys. Rev. Lett.* **28**, 449 (1972).